A novel electrochemical sensor based on LDH / CQD @ Carbon paste electrode for voltammetric determination of metronidazole in real Samples

Sakineh Alizadeh[1], Mahsa Hasanzadeh[2*]
[1]Faculty of Chemistry, Bu-Ali Sina University, Hamadan 65178638695, Iran
[2]Young Researchers and Elite Club, Tabriz branch, Islamic Azad University, Tabriz Iran

Abstract
In this work, it has been investigated the electrochemical behavior of metronidazole (MTZ) on the layer double hydroxide (LDH)/ carbon quantum dots (CQD) @ carbon paste electrode (LDH / CQD @ CPE). The ability of the proposed electrode to detect trace amounts of MTZ was evaluated by differential pulse voltammetry (DPV) technique. Different methods such as X-ray diffraction (XRD), scanning electron microscopy (SEM), cyclic voltammetry (CV), and DPV were employed to study the performance of LDH / CQD @ CPE. The effects of pH, time and accumulation potential on the voltammetric response of MTZ have studied. A liner relation between cathodic peak current and the concentration of MTZ has been shown in the range of 1.5 - 300.0 (μmol L^{-1}) with the detection limit of 2.0×10^{-1} μ mol L^{-1} under the optimum condition. The proposed method was also successfully applied for the detection of MTZ concentration in human serum and urine samples.

Index Terms: Differential Pulse Voltammetry, Metronidazole, LDH / CQD@ CPE, Sensor, Cyclic Voltammetry, Real Sample Analysis.

1 INTRODUCTION

One of the steps in drug quality control with great influence on public health, is drug analysis. Therefore, it is essential essential to develop a facile, sensitive, and precise method method for detecting active ingredients in pharmaceutical products [1]. Metronidazole (MTZ) (2-methyl-5-nitroimidazole-1-ethanol) is a member of nitroimidazole drugs mainly prescribed for treating infections caused by susceptible organisms, especially protozoa (Treponema, Trichomonas, and Histomonas) and anaerobic bacteria (Campylobacterium, Fusobacterium, Bacteroides, and Clostridium) [2, 3]. When its concentration in serum is in the range of 2 to 8 mg mL-1, it can destroy or block majority of anaerobic bacteria [4]. MTZ is the preferred drug for treating prophylaxis, Crohn's disease, and ulcerative colitis to prevent infectious complications, due to its low cost, rapid bacterial destruction, high antimicrobial activity, favorable tissue penetration, and limited adverse ejects [5, 6]. This drug had desirable pharmacokinetic and pharmacodynamic characteristics and it could be taken as topical, intravenous, oral, and vaginal formulations. If taken orally, MTZ is well absorbed and reaches its peak plasma concentration in 1-2 h [2, 5].

High performance liquid chromatography (HPLC) [7–9], titrimetry [10], and spectrophotometry [11] are commonly employed in the detection of MTZ in pharmaceutical samples. However, the majorities of these techniques are costly, tedious, time-consuming, and environmentally unfriendly and need skilled experts [12]. Accordingly, electroanalytical techniques seem to be promising due to their simplicity, rapid response, high sensitivity, ease of miniaturization, and low cost. They are also advantageous in detecting electroactive species due to due their abovementioned advantages [13, 14]. To the best of our knowledge, very few works have been published on the electrochemical determination of MTZ in pharmaceutical

and clinical samples [15-19]. Due to their extraordinary characteristics, nanomaterials have attracted great attention in this field. Nanoparticles (NPs) act as conduction centers and therefore facilitate the transfer of electrons providing high active catalytic surface area. In recent years, a wide variety of nanomaterials have been employed for modifying electrode surfaces, enhancing response signal, increasing sensitivity, and improving reproducibility [20–23]. Because organic-inorganic hybrid materials perform better than their counterparts, they have found wide applications in different technological and scientific areas. This is also due to the fact that their characteristics can be adjusted for specific application such as photochemical reactions, photochromic coatings, selective optical transmissions, etc. LDHs or hydrotalcite-like materials have been proposed as inorganic hosts for the fabrication of organic-inorganic hybrid nanolayered composites, so-called nanocomposite materials, [24].

The characteristics of CQDs are determined by their structures and components. High number of carboxylic moieties on CQD surface result in their excellent water solubility and biocompatibility [25]. They are also prone to chemical modification and surface passivation using a wide variety of organic, inorganic, polymeric, and biological materials. Surface passivation can improve the fluorescence and physical properties of CQDs. As novel fluorescent NPs, CQDs have been employed in bioimaging and biosensing due to their excellent biocompatibility and environmentally friendliness [25]. High quantum yields are needed to outperform conventional semiconductor quantum dots. Having the advantages of low toxicity and good biocompatibility, CQDs are excellent candidates to be used in bioimaging, biosensing, and drug delivery [26]. Due to their superb optical and electronic properties, CQDs can also be employed in catalysts, sensors, and optronics.[26]

In this work, we have reported a novel method for the identification of MTZ based on LDH / CQD. Once MTZ was accumulated on the surface of the modified CPE, measured using DPV and CV electrochemical techniques. Compared with bare CPE, LDH @ CPE and LDH / CQD @ CPE significantly enhanced the reduction peak of MTZ. A novel procedure with rapid response, low detection limit, low cost, and excellent reproducibility has been suggested for the determination of MTZ. Different electrochemical mechanisms of MTZ are depicted in Scheme 4. The proposed sensor was successfully employed for detecting MTZ in urine and blood serum samples.

2 Experimental

2.1 Materials

All reagents and materials used in the experiments were purchased from Merck (Darmstadt, Germany) and used as received. All chemicals were of analytical grade. 1.0×10^{-3} mol L^{-1} MTZ (Scheme 1) stock solutions were prepared daily and dilute solutions were prepared by serial dilution using doubly distilled water (DDW). A phosphate buffer solution (PBS) of pH 9.0 was used as supporting electrolyte solution.

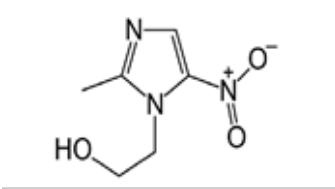

Scheme1. MTZ structure

2.2 Instrumentation

The measurements were performed with 757 VA Computrace software (Metrohm) under windows XP operating system. Three-electrode electrochemical system was consisted of CPE (modified or unmodified) as working electrode, saturated SCE reference electrode, and a Pt wire as counter electrode. A 40 kHz universal ultrasonic cleaner water bath (RoHS, Korea) was used for cleaning. The size, morphology, and composition of the prepared NPs were investigated using scanning electron microscopy (SEM) and transmission electron microscopy (TEM). The crystalline structure of the proposed NPs was determined by an X-ray diffractometer (XRD, 38066 Riva, d/G. via M. Misone, 11/D (TN) Italy) at room temperature. A Perkin-Elmer model Spectrum GX FT-IR spectrometer using KBr pellets was used for recording the mid-infrared spectra of the prepared NPs in the region of 4000–400 cm^{-1}.

2.3 Synthesis of Zn/Al-NO_3 Hydrotalcite

We synthesized Zn/Al-NO_3 LDH using coprecipitation method with Zn^{2+}/Al^{3+} molar ratio of r = 2. Metal nitrates solutions of Al $(NO_3)_3 \cdot 9H_2O$ and Zn $(NO_3)_2 \cdot 6H_2O$ were slowly mixed by constant stirring. The titration performed by dropwise addition of aqueous NaOH (1.0 mol.L^{-1}) solution up to pH 10. To prevent or minimize the atmospheric contamination of CO_2 titration with NaOH was conducted under N_2 atmosphere. Then, the prepared mixture was mixed in an oil bath shaker (70 rpm) for 18 h and aged at 70∘C. The obtained precipitate was centrifuged, washed with deionized water several times, and dried in oven at 70∘C for 2 days [27]. Then, the obtained nanocomposite was ground into a

fine powder and stored in sample containers.

2.4. Synthesis of carbon quantum dots using red Rose

Rose petals were used as carbon source for the fabrication of CQDs. To do so, red rose petals were dried in an oven at 61ºC for one day and were then ground into powder. The resulted powder was solved in 11mL DDW and lasted for 11 minutes. Then, in oven-coated mango wort, 5 g P_2O_2 was mixed with 11 mg red rose petal powder and was kept for 11 minutes where the color of the solution was changed from red to brown. Then the solution was centrifuged for 5 minutes at 5111 rpm for smoothing [28].

2.5. Surface preparation and modification

Raw and modified CPEs were fabricated using insulin syringe. The surface of the prepared electrode was smoothed on a piece of weighing paper and was regenerated after each use by pushing the paste out of the tube, removing the excess, and polishing the surface of the electrode mechanically.

2.6. Preparation of real samples

Human blood samples were obtained from healthy volunteer donors from Imam Khomeini hospital (Urmia City, Iran). The samples were centrifuged at 2500 rpm for 10 min and were kept at 4 °C until phase separation was accomplished. Serum samples were stored in freezer at −30 °C until measurement. 300 µL aliquots of each serum sample were transferred into a 25 mL volumetric flask and were diluted to the final volume of 25 with DDW. 10 ml of the prepared sample was centrifuged at 2000 rpm for 20 min. The supernatant was filtered using a filter paper with pore-diameter of 0.45 µm and then diluted five times with Birinton-Rabinson (B-R) buffer solution at pH 9.0. The obtained solution was transferred into voltammetric cell for analysis without further treatment. Standard addition method was used for measuring MTZ in the sample.

2.7. Analytical procedure

Unless otherwise stated, 0.1 mol. L^{-1} PBS at pH 8.0 was used as supporting electrolyte in all MTZ determination experiments. The solution was deaerated with N_2 gas for 10 min, and accumulation step was performed under open-circuit while stirring for 2 min. Then, DPVs (0.2 to -0.8V) or CVs (0.0 to -1.20V) of the solutions were recorded after 10 s quiet time. Cathodic peak currents were measured at −0.4 in DPVs or −0.48V in CVs.

3 RESULT AND DISCUSSION

3.1. Characterization of LDH / CQD @ CPE

TEM and TGA (thermo-gravimetry analysis) of Zn-Al (NO_3) -LDH was recorded and is depicted in Fig. 1(A, B) which showed particles with the size of 84 nm and number of water of LDH respectively. Fig. 2 (A, B, C) shows SEM, XRD pattern and FT-IR spectrum of Zn–Al $(NO_3)^-$ LDH. The characteristic reflections of (0 0 3), (0 0 6), (0 0 9) planes of crystalline LDH can be clearly observed in the figure. The typical doublet of (1 1 0)–(1 1 3) planes in LDH was also observed. It can be seen that Zn–Al (NO_3^-) LDH exhibited only the characteristic reflections of hydrotalcite-like LDH with no other crystalline phases which complied with previously reported results [29]. The nature and symmetry of interlayer anions and the presence of impurity were investigated using infrared absorption spectroscopy. The absorption band at about 3446 cm^{-1} in the FT-IR spectrum of Zn–Al (NO_3^-) LDH (Fig. 2C) was assigned to the stretching vibration of hydroxyl groups on LDH layers and interlayer water molecules. The weak band at 1631 cm^{-1} was due to the bending mode of water molecules. The band with maximum peak at 1379.01 cm^{-1} was attributed to the stretching vibration of NO_3^- ions intercalated in the interlayer gallery. Finally, the bands at 607, 557.39 and 428.17 cm^{-1} were assigned to M–O stretching modes and M–O–H bending vibrations [30].

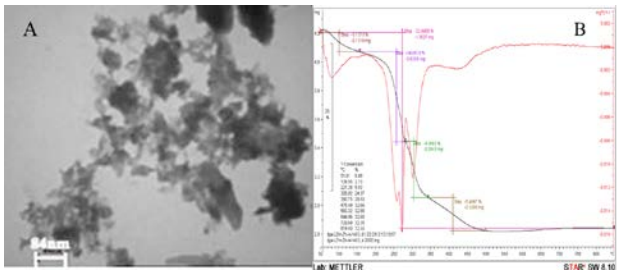

Fig.1. A) TEM image and B) (TGA) thermogravimetric curves of Zn-Al(NO_3)- LDH (60ºC, pH 9, mole ratio 2: 1, and water as solvent, 0.131 mg sample mass reduction by increasing temperature from room temperature up to 150 ° C).

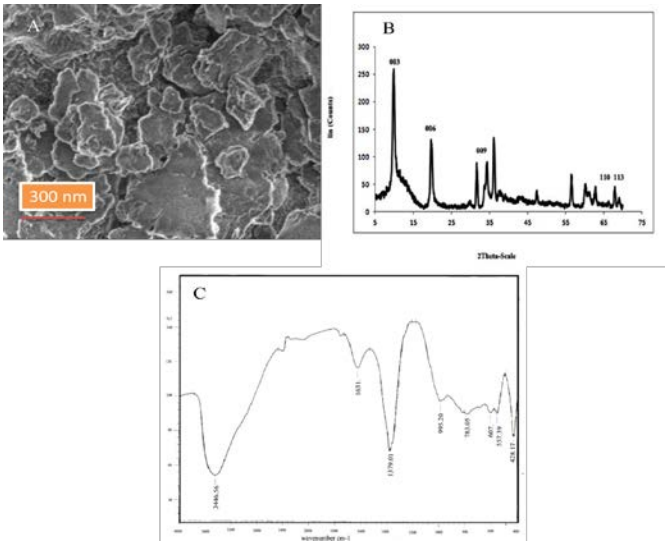

Fig.2. A) SEM, B) XRD and C) FTIR spectrum of Zn-Al (NO_3) - LDH at 120 ° C, pH 9 mole ratio of 2: 1, and water as solvent, 1-propanol and ethylene glycol.

Scheme 2. Structure of CQDs

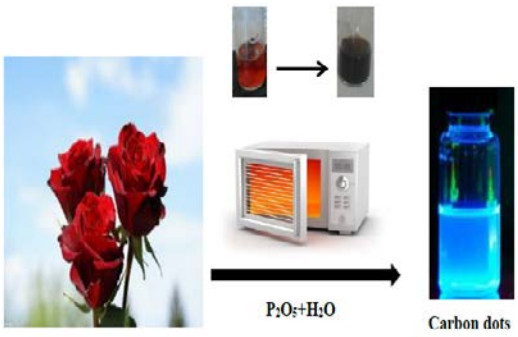

Scheme3. Schematic of CQDs synthesis

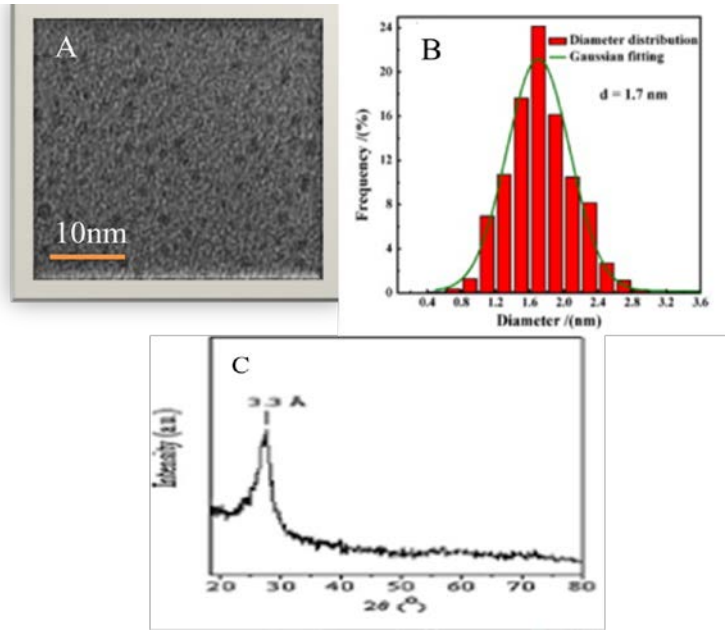

Fig.3. A) TEM image, B) DLS and C) XRD pattern of CQDs synthesized from red rose.

In Fig 3 (A, B, C) it can showed the TEM image of CQDs (Scheme 2, 3) and DLS and XRD of these nanoparticles. Also in Fig 4(A, B, C) the surface morphology of LDH / CQD @ CPE, a scanning electron microscope was employed. SEM images of the modified electrode confirming the distribution of LDH and CQD on the surface of the electrode without aggregation with specific three-dimensional structures. The distribution of NPs was also observed in the SEM image of LDH / CQD @ CPE providing a large surface area for the electrode.

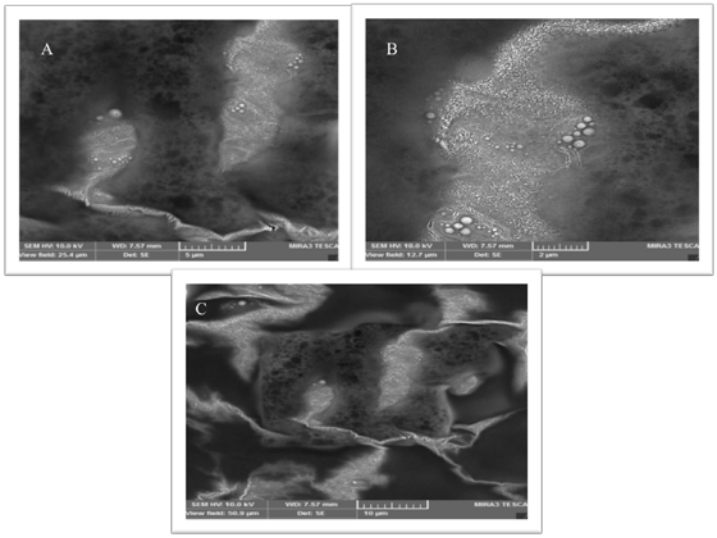

Fig.4. A, B, C) SEM image of Zn-Al (NO_3) – LDH/ CQDs @ CPE .

3.2. Voltammetric behavior of MTZ at LDH / CQD @ CPE

To investigate the catalytic activity of LDH / CQD @ CPE in the determination of MTZ, DPVs of the samples were recorded in the potential range of 0.2 to -0.8 vs. SCE in PBS at pH 8.0 as the background electrolyte. Significant increase in current response with decrease in peak potential indicated that in LDH / CQD @ CPE, NPs acted as assistant mediator in the electrochemical reaction, essentially accelerating the rate of electron transfer. The obtained voltammograms are shown in Fig. 5. A sharp peak was observed at about -0.4 V vs. SCE [31]. The DPVs recorded for MTZ (120 µmol L^{-1}) on bare CPE, LDH @ CPE, and LDH / CQD @ CPE are shown in Fig. 5. The lowest MTZ reduction signal was obtained on bare CPE. LDH / CQD @ CPE showed higher current density compared with CQD @ CPE due to its higher surface area and the catalytic effects of LDH and CQD NPs. On LDH / CQD @ CPE, MTZ was irreversibly reduced at pH 8.0 giving a reduction peak initiating in the negative direction. Under similar conditions, a weak peak was observed on bare CPE. As can be seen, the values of the cathodic peak currents of MTZ on CQD @ CPE and LDH / CQD @ CPE were higher than that on bare CPE. LDH nanocomposite increased the effective surface area of the electrode which in turn enhanced the electrochemical properties of the modified electrode and LDH @ CPE increased the surface area of the electrode and also provided a good surface for electron transfer.

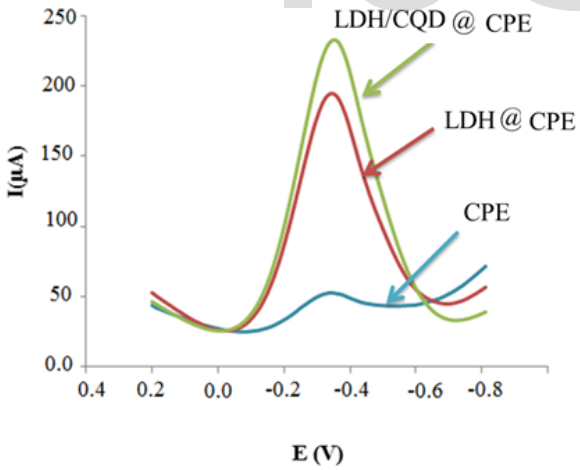

Fig. 5. DPV for bare GCE, LDH @ CPE and LDH/ CQDs @ CPE from below in optimum condition (120 µmol. L^{-1} MTZ).

3.3. Influence of pH

We also investigated the effect of pH on the cathodic peak current and peak potential of MTZ on LDH / CQD @ CPE. PBS solutions with pH values of 2.0 on 12.0 were employed to investigate the effect of pH on the determination of MTZ at LDH / CQD @ CPE. The obtained results showed that voltammetric responses strongly depended on pH in the acidic and neutral pH media, but this was not the case in alkaline medium which complied with most of the electrochemical methods reported previously. pH-independent peak potential in alkaline medium could be due to the unavailability of protons required for the reduction of MTZ at pH values above its pka value. Fig. 6 shows the CVs obtained for 120µ mol. L^{-1} MTZ where its reduction is pH dependent (pHs 2.0–8.0). A sharp irreversible cathodic peak was witnessed on CPE in all tested buffers. The effect of pH on peak current was also investigated (Fig. 6A). Cathodic peak current was sharply increased from pH 2.0 to 8.0 but above that it was decreased. Therefore, pH 8.0 was chosen as the optimum pH for subsequent experiments which complied with previous works [16].

By increasing the pH of the solution up to 8.0, a shift in peak potential towards negative direction was witnessed indicating the involvement of protons in the reduction of MTZ in acidic and neutral media (Fig. 6). this trend was in agreement with previously reported works [32].

A linear relation between peak potential and solution pH was observed in the pH range of 2.0–8.0 (Fig. 6C) with linear regression equation and correlation coefficient of $E\ PC$ (mV) = −189.6− 26.5 pH and r = 0.9903, respectively. The observed slope of 26.5mV/pH suggested that the number of protons involving in the reaction was similar to the number of electrons participating in the rate determining step. Therefore, a reaction mechanism involving four electrons and four protons was proposed (Scheme 4).

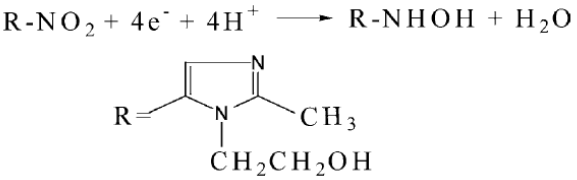

Scheme 4. mechanism of MTZ reduction.

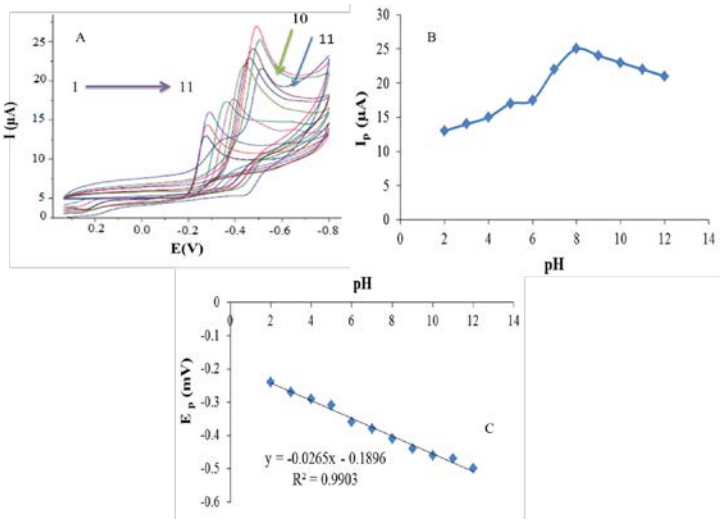

Fig. 6. Influence of pH on the cathodic peak current and cathodic peak potential of 120 µmol.L^{-1} MTZ in the range of 2.0-12.0.

3.4. Effect of Scan Rate

We evaluated the effects of scan rate on the reduction peak current and peak potential of MTZ. Fig. 7 show the cyclic voltammogram of 120 µ mol. L^{-1} MTZ at scan rate of 10–250 mV/s. The shift of cathodic peak potential to more negative values verified the irreversibility of the reduction of MTZ on LDH / CQD @ CPE [33]. In order to investigate whether the reduction of MTZ on LDH / CQD @ CPE was predominantly diffusion or adsorption controlled, correlation coefficients of linear plots of reductive peak currents versus scan rate as well as reductive peak current versus square root of scan rate were compared (Fig. 7 B and C). On the other hand, a better correlation coefficient was obtained for the dependence of reductive peak current on the scan rate (r = 0.9927) compared to the square root of scan rate (r = 0.95) indicating that the reduction of MTZ on LDH / CQD @ CPE was controlled by both surface-adsorption and diffusion kinetics but surface confined kinetics was more effective [34].

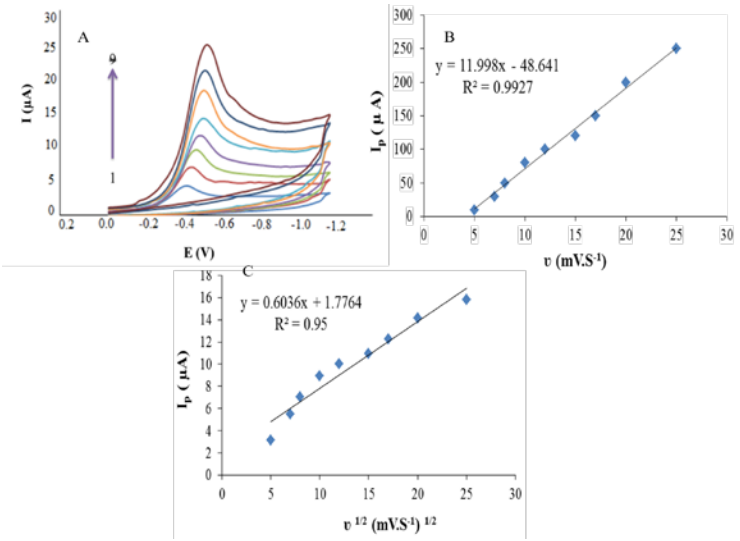

Fig. 7. A) CV for effect of scan rate and in optimum condition at concentration of 120 µmol L $^{-1}$ MTZ (B) effect of I_p Vs. U and C) I_p Vs. $U^{1/2}$.

3.5. Evaluation of method performance

(µA) = Y = 4.9242 x+5.1844, R^2 = 0.9998. Limit of detection was defined as LOD = 3 S_b/m where S_b and m are standard deviation of blank and the slope of calibration graph, respectively, which was calculated to be 0.2 µmol L^{-1} for the modified electrode.

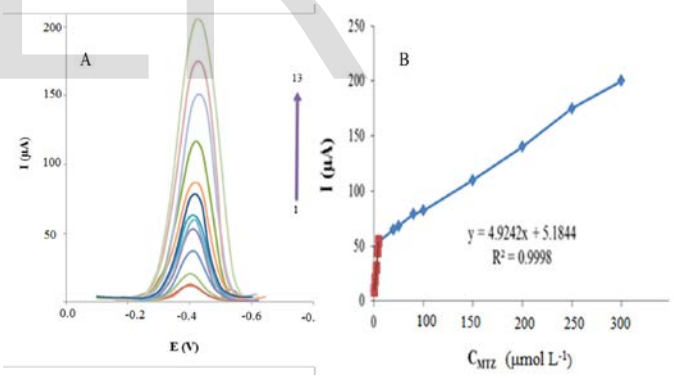

Fig. 8. DPVs for 1.5-300 µmol L^{-1} MTZ at LDH/ CQDs @ CPE in 0.1 mol L^{-1} PBS (pH 8.0), B) show the plots of the peak current as a function of MTZ concentration in the range of 1.5-300 µmol L^{-1}.

The repeatability of the electrode in the determination of MTZ was investigated by conducting six measurements with the same MTZ standard solution using the same electrode. Relative standard deviations (RSD) for 100.0, 150.0, and 200.0 µmol L^{-1} solutions were obtained to be 1.08, 1.09, and 1.78%, respectively. The reproducibility of the electrode response was also investigated. Five electrodes were fabricated using the same batch and were evaluated by measuring 100.0 µmol L^{-1} MTZ standard solution. The RSD of the responses ob-

tained from different electrodes was 2.28% for the LDH/CQD @CPE. The obtained results showed that the modified electrode had acceptable repeatability and reproducibility in the detection of MTZ. To study the storage stability of the proposed electrode, the electrode was stored at room temperature for 5 weeks, then the current peak of the reaction was recorded with the stored electrode and the obtained response was compared with that obtained before storing. Therefore, we concluded that LDH/CQD@CPE had high stability. High reproducibility and stability of the proposed electrode showed that it could be applied for the analysis of real samples.

3.6. Interference study

To investigate the selectivity of the proposed method in the determination of MTZ, the effect of potentially interfering species on the detection of analytes was studied. Tolerance limit of interfering species was defined as the maximum concentration with relative error of less than 75.0% at MTZ concentration of 200 μmol L^{-1}. As summarized in Table 1, no current response was observed for the studied compounds. In this experiment, the oxidation of biomolecules such as lysine, asparagine, cysteine, glutamine, tyrosine, valine, rabeprazole, omeprazole, and tinidazole could interfere with the oxidation of MTZ; however, LDH/CQD@CPE successfully solved this problem. Also, Ce^{2+}, Cd^{2+}, Zr^{2+}, Co^{2+}, Pb^{2+}, Ag^{+}, Zn^{2+}, Na^{+}, Al^{3+}, Mg^{2+}, NH_4^{+}, Hg^{2+}, Fe^{3+}, Ni^{2+}, Se^{4+}, Li^{+}, NO_3^{-}, SO_4^{2-}, and Cl^{-} did not interfere with the I_p of MTZ at concentrations of up to 1000 times that of MTZ. This verified that common interfering species did not significantly affect the detection of MTZ in pharmaceutical and biological samples on LDH/CQD@CPE.

Table 1 Effect of interfering species

Interfering ions	Tolerable concentration (analyte: interfering ion)[a, b]
Rabeprazole, Omeprazole, Tinidazole	1:100
Lysine, cysteine, asparagine, ,glutamine valine, tyrosine	1:500
Cd^{2+},Ce^{2+},$Zr^{2+}$$Ag^{+}$,$Co^{2+}$,$Zn^{2+}$,$Pb^{2+}$, Na^{+} ,NH_4^{+},Al^{3+}, Mg^{2+}, Fe^{3+},Se^{4+},Hg^{2+}, Li^{+}, Ni $^{2+}$, NO_3^{-},SO_4^{2-},Cl^{-}	1:1000

a Concentration of analyte is 200 μmol L^{-1}
b At this ratio no interfering effect was observed

3.7. Real sample analysis

The applicability of the prepared sensor was evaluated by detecting MTZ in human urine and serum samples. Once the sample was prepared and diluted to desirable concentrations as described earlier, DPV was applied to measure MTZ in human serum and urine samples. MTZ was also measured after it was added into human urine and serum samples and corresponding recovery values were calculated. The obtained results were between 98.3 to 103.5% which was acceptable and are summarized in Table 2. Comparison of the results obtained for the determination of MTZ by a variety of modified electrodes and analytical parameters reported in the literature [35–43] are given in Table 3. The comparative data verified the superiority of the proposed sensor over some previously reported methods, especially in terms of detection limit and sensitivity. This was due to the immobilization of LDH/CQD composite on CPE with large surface area and excellent conductivity.

Table 2 . Determination of MTZ in human serum and urine samples

Samples	Added (μmol L−1)	Found (μmol L−1)	Recovery(%)
Human serum	0.0	0.0	–
	50	49.23	98.46
	100	98.3	98.3
	150	148.515	99.01
Human urine	0.0	0.0	-
	50	50.51	101.02
	100	101.1	101.1
	150	153.045	102.03
	180	186.3	103.5

Table 3 Characteristic performance data obtained by electrochemical method and other techniques for determination of MTZ

Detection method	Linear range (μmol L^{-1})	LOD (μmol L^{-1})	Reference
Coated GCE (CV)	70-800	2.3	35
DNA/GCE (CV)	0.1-6	0.02	36
Gr-IL/GCE (CV)	0.1-2.5	0.01	37
Au electrode (CPP)	20-800	0.15	38
3D GNE (SWV)	0.01-2	0.001	39
MIS-CPE (DPSV)	1-100	0.036	40

Cu-poly(Cys)/GCE (LSV/CV)	0.5-400	0.37	41
MMIP/MGCE (CV/EIS)	0.05-1	0.016	42
Activated GCE (LSV)	2-600	1.1	43
LDH/CQD@CPE	1.5-300	0.2	This work

4. Conclusion

LDH/CQD modified CPE showed good voltammetric response in the detection of MTZ in aqueous solutions. This is important since the nitro group on MTZ, which acts as an electroactive reducible center, has poor reproducibility and sensitivity on bare electrodes. CV and DPV measurements of MTZ on LDH/CQD@CPE showed irreversible reduction peaks in the studied potential range. While the shift of peak potential with scan rate verified that the reaction was irreversible, the shift of peak potential with pH revealed the involvement of protons in the reduction reaction. Under the optimized solution pH and accumulation parameters, the modified CPE showed a wide linear range with comparable LOD, recovery, and selectivity to previously reported works obtained with expensive electrodes.

Acknowledgement

The authors acknowledge Bu-Ali Sina University Research Council and Center of Excellence in Development of Environmentally Friendly Methods for Chemical Synthesis (CEDEFMCS) for providing support to this work.

References

[1] Mashhadizadeh MH, Rasouli F (2014) Design of a new carbon paste electrode modified with TiO2 nanoparticles to use in an electrochemical study of codeine and simultaneous determination of codeine and acetaminophen in human plasma serum samples, Electro anal. 26: 2033–2042.

[2] Edwards D I (1993) Nitroimidazole drugs—action and resistance mechanisms I. Mechanisms of action," J. Of Antimicrob.Chemothera. 31:9–20.

[3] Verma P, Namboodiry V, Mishra S, Bhagwat A, Bhoir S (2013) A stability indicating HPLC method for the determination of Metronidazole using Ecofriendly solvent as mobile phase component, Int. J. Of Pharm. and Pharmaceut. Sci. 5: 496–501.

[4] Pendland S L, Piscitelli S C, Schreckenberger PC, Danziger LH (1994) In vitro activities of metronidazole and its hydroxyl metabolite against Bacteroides spp, Antimicrob.Agents and Chemother. 38: 2106–2110.

[5] Wild GE (2004) the role of antibiotics in the management of Crohn's disease, Inflame. Bowel Diseas. 10: 321–323.

[6] Mark SL, Edlund C, Nord CE (2010) Metronidazole is still the drug of choice for treatment of anaerobic infections, Clin. Infect. Diseas. 50: S16–S23.

[7] Gulaid A, Houghton GW, Lewellen O RW, Smith J, Thorne PS(1978) Determination of metronidazole and its two major metabolites in biological fluids by high pressure liquid chromatography ,Brit. J. Of Clin. Pharmacol. 6: 430–432.

[8]Ezzeldin E, El-Nahhas T M (2012) New analytical method for the determination of metronidazole in human plasma: application to bioequivalence study, Trop. J. Of Pharmace. Res., 11:799–805.

[9]Thulasamma P, Venkateswarlu P (2009) Spectrophotometric method for the determination of metronidazole in pharmaceutical pure and dosage forms, Rasayan J. of Chem.2: 865–868.

[10] Manohara YN, Venkatasha R, RevathiBahlul R, Awen Z (2010) Novel and rapid estimation of metronidazole in tablets, Der Pharma Chemica. 2: 148–151.

[11]Threresa JC, Minju R, Reshma K R, Vidya TV, Vrinda PS, Vrindha T N (2014) Spectrophotometric determination of metronidazole in bulk and dosage form, Int. J. Of Pharm. and Pharmace. Sci. 1:11–15.

[12] Siddiqui MR, Alothman ZA, Rahman N(2013)Analytical techniques in pharmaceutical analysis: a review, Arab. J. Of Chem. 1:102-108

[13] La-Scalea M A, Serrano S H P, Gutz IG R(1999)Voltammetric behavior of metronidazole at mercury electrodes, J.of the Brazil. Chem. Soc. 10: 127–135.

[14] Abu Zuhri A Z, Al-Khalil S I, Suleiman MS (1986) electrochemical reduction of metronidazole and its determination in pharmaceutical dosage forms by D.C. polarography, Anal. Lett. 19: 453–459.

[15] Brett A MO, Serrano SHP, Gutz IG R, La- Scalea MA(1997)Voltammetric behavior of metronidazole at different electrodes, Electroanalysis. 9: 110–114.

[16] Sahu G (2010) Voltammetric behavior of metronidazole at a composite polymer membrane electrode, Orient. J. Of Chem. 26:81–86.

[17] Selehattin Y, Baltaoglu E, Saglikoglu G, Yagmur S, Polat K, Sadikoglu M(2013) Electroanalytical determination of metronidazole in tablet dosage form, J. Of the Serb. Chem. Soc. 78: 295–302.

[18] Ozkan S A, Ozkan Y, Senturk Z (1998) Electrochemical reduction of metronidazole at activated glassy carbon electrode and its determination in pharmaceutical dosage forms, J.of Pharmaceut. and Biomed. Anal. 17, no. 2, pp. 2:99– 305.

[19] Lu S, Wu K, Dang X, Hu S (2004) Electrochemical reduction and voltammetric determination of metronidazole at a na-

nomaterial thin film coated glassy carbon electrode, Talanta. 63: 653–657.
[20] Songa H, Nia Y, Kokot S (2013) a novel electrochemical biosensor based on the hemin–
Graphene nano-sheets and Au nano-particles hybrid film for the analysis of hydrogen
Peroxide, Anal. Chim. Acta. 788: 24–31.
[21] Liu X, Luo L, Ding Y, Kang Z, Ye D (2012) Simultaneous determination of L-cysteine and L-tyrosine using Au-nanoparticles/poly-eriochrome black T film modified glassy carbon
electrode, Bioelectrochem. 86:38–45.
[22] Yang Y, Fang G, Liu G, Pan M, Wang X, Kong L, He X, Wang S (2013) Electrochemical
sensor based on molecularly imprinted polymer film via sol–gel technology and
multi-walled carbon nanotubes–chitosan functional layer for sensitive determination
of quinoxaline-2-carboxylicacid, Biosens. Bioelectron. 47:475–481.
[23] Yan J, Liu S, Zhang Z, He G, Zhou P, Liang H, Tian L, Zhou X, Jiang H (2013) Simultaneous electrochemical detection of ascorbic acid, dopamine and uric acid based on
graphene anchored with Pd–Pt nanoparticles, Colloids Surf. B 111:392–397.
[24] Hussein M Z B, Yahaya A H, Shamsul M, Salleh H M, Yap T, Kiu J (2004) Acid fuchsin-interleaved Mg-Al-layered double hydroxide for the formation of an organic-inorganic hybrid nanocomposite, Materials Lett. 58: 329–332.
[25] Wang Y, Hu A (2014) Carbon quantum dots: Synthesis, properties and applications, J. of Materials Chem. C. 2: 6921–39.
[26] Ying L S, Wei Sh, Zhiqiang G (2015) Carbon quantum dots and their applications, Chem. Soci. Rev. 44: 362–365.
[27] Cao F, Wang y, Ping Q, Liao Z (2011) Zn-Al-NO_3-Layered double hydroxides with intercalated diclofenac for ocular delivery, Int. J.of pharmacy. 404: 250-256.
[28] Feng Y, Zhong D, Miao H, Yang X (2015) Carbon dots derived from rose flowers for tetracycline sensing, Talanta. 140:128–133.
[29] Pisson J, Taviot C, Besse J P, Morel JP (2003) Intercalation of dicarboxylate anions in to a Zn-Al-Cl layered double hydroxide: microcalorimetic determination of the enthalpies of anion exchange, J. Mater. Chem. 13: 2582-2585.
[30] Saber O, Tagaya H (2008) preparation and interealation reactions of nano-structural materials, Zn-Al-Ti LDH, Mater. Chem. Phys.108: 449-455.

[31] Shahnazari-Shahrezaieab E, Nezamzadeh-Ejhieh A (2017) A zeolite modified carbon paste electrode based on copper exchanged clinoptilolite NPs for voltammetric determination of MTZ, RSC. Adv. 7: 14247-14255.

[32] Wang Y, Xu H, Zhang J, Li G (2008) Electrochemical sensors for clinic analysis, Sensors. 8: 2043–2081.
[33] Wang J (2006) Analytical Electrochemistry, John Wiley & Sons, New Jersey, NJ, USA, 3rd edition.
[34] Brett C M A, Brett A M O (1993) Electrochemistry Principles, Methods, and Applications, Oxford University Press, Oxford, UK, 1st edition.
[35] Li C, Zheng B, Zhang T, Zhao J, Gu Y, Yan X, Li Y, Liu W, Feng G, Zhang Zh (2016) homogeneously dispersed multimetal oxygen- evolving catalysts, RSC Adv. 6:45202–45209.
[36] Jiang X, Lin X (2006) fabrication of a nanobiocomposite film containing heme proteins and carbon nanotubes on a choline modified glassy carbon electrode, Bioelectrochem. 68: 206–212.
[37] Erk N (2003) differential pulse anodic voltammetric determination of pantoprazole in pharmaceutical dosage forms and human plasma using glassy carbon electrode, Anal. Biochem. 323: 48–53.
[38] Rezaei B, Damiri S (2010) fabrication of nanostructure thin film on the gold electrode using continuous pulsed-potential technique and its application for electrocatalytic determination of metronidazole, Electrochim. Acta. 55:1801–1808.
[39] Mollamahale YB, Ghorbani M, Ghalkhani M, Vossoughi M, Dolati A (2013) highly sensitive 3D gold nanotube ensembles: application to electrochemical determination of metronidazole, Electrochim. Acta, 106: 288–292.
[40] Hu C, Deng J, Xiao X, Zhan X, Huang K, Xiao N, Ju S (2015) determination of dimetridazole using carbon paste electrode modified with aluminum doped surface molecularly imprinted siloxane Electrochim. Acta. 158: 298–305.
[41] Gu Y, Yan X, Liu W, Li C, Chen R, Tang L, Zhang Zh, Yang M (2015) nanostructured Mo-based electrode materials for electrochemical energy storage, Electrochim. Acta. 152:108–116.
[42] Chen D, Deng J, Liang J, Xie J, Hu C, Huang K (2013) a core-shell molecularly imprinted polymer grafted onto a magnetic glassy carbon electrode as selective sensor for determination of metronidazole, Sens. Actuators. B. 183: 594–600.
[43] Ozkan SA, Ozkan Y, Senturk Z (1998) electrochemical reduction of metronidazole at activated glassy carbon electrode and its determination in pharmeutical dosage forms, J. Pharm. Biomed. Anal. 17: 299–305.